Control-relevant nonlinearity measure and integrated multi-model control

Jingjing Du [a,*], Tor Arne Johansen [b]

[a] College of Internet of Things Engineering, Hohai University, Changzhou 213022, China

[b] Department of Engineering Cybernetics, Norwegian University of Science and Technology, NO 7491 Trondheim, Norway

Abstract: A control-relevant nonlinearity measure (CRNM) method is proposed based on the gap metric and the gap metric stability margin to measure the nonlinear degree of a system once a linear control strategy is selected. Supported by the CRNM method, an integrated multi-model control framework is developed, in which the multi-model decomposition and local controller design are closely integrated, model redundancy is avoided, computational load is reduced, and dependency on a prior knowledge is reduced. Besides, a $1/\delta$ gap-based weighting method is put forward to combine the local controllers. On one hand, the $1/\delta$ gap-based weighting method has merely one tuning parameter and can be computed off-line; on the other hand, it is sensitive to the tuning parameter, flexible and easy to tune. Two continuous stirred tank reactor (CSTR) systems are investigated. Closed-loop simulations validate the effectiveness and benefits of the proposed integrated multi-model control approach based on CRNM.

Keywords: control-relevant nonlinearity measure, gap metric, weighting method, integrated multi-model control, CSTR

1. Introduction

Virtually all chemical processes are nonlinear. However, most of them are handled using linear analysis and design techniques because of operating around an equilibrium point, so that the development and implementation of a controller can be largely simplified [1]. Nevertheless, in some important cases, the linearity assumption does not hold and linear controllers are invalid. Then nonlinear controllers are necessary. Therefore, from the perspective of controller design, there is a need for nonlinearity measures, which quantify the nonlinearity extent of a process instead of merely judging a system as linear or nonlinear. Thus we can decide whether a linear controller is adequate for the system or a nonlinear controller is necessary according to the nonlinearity measures. In the past decades, researchers have made extensive studies on nonlinearity measures, and have proposed quite a few definitions and computational methods [1-13]. Most of them are defined as a distance between the nonlinear system and its best linear approximation [2-9]. Although the definitions are intuitive, the general computation of the best linear models and nonlinearity measures are rather complicated [2]. Besides, most of them cannot be used in feedback controller synthesis directly [3].

Recently, the gap metric which was recognized as being more appropriate to measure the distance between two linear systems than a norm-based metric [17-18], has been employed to quantify the nonlinearity level of industrial processes. And several definitions have been developed [13-16]. The nonlinearity measures based on the gap metric are comparatively easier and simpler to compute and apply. And some of them have been used for multi-model decomposition in the multi-model control framework [15, 16].

The multi-model control approaches have been popular in controlling chemical processes

with wide operating ranges and large set-point changes [19-37]. The key point is to decompose a nonlinear system into a set of linear subsystems, so that classical linear control strategies can be easily adopted. Generally, the multi-model control approaches comprise three elements: the multi-model decomposition (*i.e*., model bank determination), the local controller design, and the local controller combination. From an integration perspective, it is necessary to connect the three elements closely, so that local model redundancy can be avoided to simplify the controller structure, dependency on previous knowledge can be reduced to make the design procedure more systematic, computational load can be decreased to make the method more efficient, and performance of the controller can be raised to make the method more effective. Therefore, integrated multi-model control methods have been recently put forward [19, 28-30], in which the model bank determination, the local linear controller design, and the local linear controller combination are fully or partly integrated. Two integrated multi-model control design frameworks were proposed in Ref. [19]. One method (Algorithm 2) uses the maximum stability margin (which is comparatively controller-independent) while the other (Algorithm 1) uses the actual stability margin of a given controller design. Although Algorithm 2 from Ref. [19] is simpler, it has a tuning parameter which depends on a priori knowledge. Algorithm 1 from Ref. [19] is more systematic; however, it is more complicated and involves intensive computation and tests. In Ref. [20], a weighting method with only one tuning parameter was proposed based on the gap metric, in which the weights can be computed off-line and kept in a look-up table. Here we call it 1-δ method for simplicity. It is intuitive and simple compared to traditional methods. Therefore, Ref. [29] used it to connect the local controller combination with the other two steps to propose an integrated multi-linear model predictive control method. However, the 1-δ method is not sensitive to the tuning parameter, which is undesirable.

In this paper, a control-relevant nonlinearity measure (CRNM) method is proposed to quantify the nonlinearity extent of a process based on the gap metric, which can be used directly in controller synthesis: It offers guidance for controller design; and it sets up a criterion to assess the controller's performance. The proposed CRNM method is then employed to perform model bank determination and local controller design in a multi-model control framework. Besides, a 1/δ gap-based weighting method, which has all the advantages of the 1-δ method and is more sensitive to the tuning parameter, is put forward to combine the local controllers. Thus an improved integrated multi-model control framework is established based on CRNM, which integrates the advantages of the algorithms Ref. [19] while overcomes their disadvantages. The proposed integrated multi-model control approach aims to realize four goals. (a) To select as few linear models as necessary to design a multi-model controller, so that the model redundancy can be avoided; (b) to use as little a priori knowledge as possible, so that the method can be systematic and user-friendly; (c) to reduce computational load as much as possible, so that the method can be easy to implement; (d) to schedule the local controllers as well as possible so that the global multi-model controller can be more effective. Two CSTRs are simulated to illustrate the use of the improved integrated multi-model control approach. Simulation results demonstrate that the proposed CRNM-based integrated multi-model framework is systematic, efficient and effective, and performs better than related multi-model control methods [20, 26].

This paper is organized as follows. Related background about the gap metric and the gap metric stability margin is shortly reviewed in Section 2. In Section 3, a control-relevant nonlinearity measure method is proposed. Supported by the proposed nonlinearity measure, an

integrated multi-model control approach is proposed in Section 4, which includes a CRNM-based multi-model decomposition and local controller design procedure and a $1/\delta$ gap-based weighting method. Closed-loop simulations are present in Section 5 to illustrate the effectiveness of the proposed approaches, and comparisons have been made with related methods. In Section 6, some conclusions are made about the paper.

2. Gap metric and gap metric stability margin

Relevant background about the gap metric and the gap metric stability margin is briefly recalled in this section.

2.1. Gap metric

The gap metric between two linear systems P_1 and P_2 with their normalized right coprime factorizations $P_1 = N_1 M_1^{-1}$ and $P_2 = N_2 M_2^{-1}$, is denoted as $\delta(P_1, P_2)$ and is defined by the maximum of two directed gaps [17]:

$$\delta(P_1, P_2) := \max\{\vec{\delta}(P_1, P_2), \vec{\delta}(P_2, P_1)\} \tag{1}$$

where $\vec{\delta}(P_1, P_2) = \inf_{Q \in H_\infty} \left\| \begin{bmatrix} M_1 \\ N_1 \end{bmatrix} - \begin{bmatrix} M_2 \\ N_2 \end{bmatrix} Q \right\|_\infty$ and $\vec{\delta}(P_2, P_1) = \inf_{Q \in H_\infty} \left\| \begin{bmatrix} M_2 \\ N_2 \end{bmatrix} - \begin{bmatrix} M_1 \\ N_1 \end{bmatrix} Q \right\|_\infty$.

The gap metric between any two linear systems is bounded between 0 and 1. Therefore, the gap metric is more intuitive than a metric based on norms. Besides, the gap metric offers some useful information for control system analysis and synthesis. For example, if the gap metric between two systems is close to 0, then at least one feedback controller can be found to stabilize both of them; otherwise if the gap is close to 1, it will be difficult of impossible to design a feedback controller that can stabilize both systems[18].

2.2. Gap metric stability margin

Suppose K is a feedback controller that can stabilize the linear system P, then the gap metric stability margin of the closed-loop system is defined as [38]:

$$b_{P,K} = \left\| \begin{bmatrix} I \\ K \end{bmatrix} (I + PK)^{-1} \begin{bmatrix} I & P \end{bmatrix} \right\|_\infty^{-1} = \left\| \begin{bmatrix} I \\ P \end{bmatrix} (I + KP)^{-1} \begin{bmatrix} I & K \end{bmatrix} \right\|_\infty^{-1} \tag{2}$$

where I is the identity matrix. The gap metric stability margin is also called the normalized coprime stability margin.

Denote the left normalized coprime factors of P as $P = \tilde{M}^{-1}\tilde{N}$, and the Hankel norm as $\| \|_H$.

Then the maximum gap metric stability margin of P is defined as [38]:

$$\begin{aligned} b_{opt}(P) &:= \left\{ \inf_{K \text{ stabilizing}} \left\| \begin{bmatrix} I \\ K \end{bmatrix} (I + PK)^{-1} \begin{bmatrix} I & P \end{bmatrix} \right\|_\infty \right\}^{-1} \\ &= \sqrt{1 - \left\| \begin{bmatrix} \tilde{N} & \tilde{M} \end{bmatrix} \right\|_H^2} < 1 \end{aligned} \tag{3}$$

From Eq. (3), it is clear that the maximum stability margin is an intrinsic property of the plant P, and has nothing to do with the controller. Besides, for the same system P, the maximum stability is greater than or equal to $b_{P,K}$ for any controller K.

The connection between the gap metric and the gap metric stability margin is shown by

Proposition 1.

Proposition 1 [38]: Suppose the feedback system with the pair (P_0, K) is stable. Let $\mathcal{P} := \{P: \delta(P, P_0) < r\}$. Then the feedback system with the pair (P, K) is also stable for all $P \in \mathcal{P}$ if and only if

$$b_{P_0,K} \geq r > \delta(P, P_0) \tag{4}$$

Once a nonlinear process is linearized around a set of equilibrium points, the gap metric and the gap metric stability margin are usable. In this work, we will use the gap metric and the gap metric stability margin to propose a CRNM method on the basis of Proposition 1. The gap metric and maximum stability margin of the system are used to define a preliminary nonlinearity measure NM_1 for guidance before a controller is designed, and afterwards the gap metric and actual stability margin of the closed-loop system are used to define a secondary nonlinearity measure NM_2 to qualify the performance of the controller. If NM_2 of the considered system is smaller than 1, it means that the linear controller is capable to stabilize it. Otherwise, we will decompose the nonlinear system into a set of linear subsystems and design a set of local linear controllers according to the nonlinearity measure criteria. Thus, the proposed CRNM method tells us whether the linear controller is capable to stabilize the nonlinear system or not.

Besides, the gap metric is also used for controller combination in the multi-model control of nonlinear systems by some researchers [20, 21]. In section 4, this work will proposed a $1/\delta$ gap-based weighting method, which is simpler and more flexible compared to existent weighting methods.

3. Control-relevant nonlinearity measures based on gap metric and gap metric stability margin

Consider a nonlinear system represented by Eq. (5):

$$\begin{cases} \dot{x} = f(x, u) \\ y = g(x, u) \end{cases} \tag{5}$$

where $x \in R^n$ is the state vector, $u \in R^r$ is the control input vector, $y \in R^m$ is the output vector, and $f(\cdot)$ and $g(\cdot)$ are nonlinear differentiable functions.

Denote the scheduling variables of system (5) by θ. Generally, θ includes a subset of the states, inputs and outputs. According to the principles of gain scheduled control design [39], θ should vary slowly, captures the nonlinearities of the system, characterizes the operating level and uniquely defines the equilibrium points of system (5).

Denote Φ as the scheduling space of plant (5), and we have $\theta \in \Phi$. Namely, Φ is the variation range of θ, also the operating space of plant (5). Then Φ is gridded through the gap metric based dichotomy method [24]. Suppose n gridding points $\theta = [\theta_1, \theta_2, \theta_i \ldots, \theta_n]$ are acquired. Then every gridding point corresponds to an equilibrium point of system (5). The operating point for θ_i is denoted as $(x_o(\theta_i)\ u_o(\theta_i)\ y_o(\theta_i)) := (x_{oi}, u_{oi}, y_{oi})$. Then system (5) is linearized about (x_{oi}, u_{oi}, y_{oi}) and a linearized model P_i is obtained described by:

$$\begin{cases} \delta\dot{x} = A_i\delta x + B_i\delta u \\ \delta y = C_i\delta x + D_i\delta u \end{cases} \quad i = 1, \ldots, n \tag{6}$$

where $\delta x = x - x_{oi}$, $\delta u = u - u_{oi}$, $\delta y = y - y_{oi}$, $A_i = \dfrac{\partial f(x_{oi}, u_{oi})}{\partial x}$, $B_i = \dfrac{\partial f(x_{oi}, u_{oi})}{\partial u}$

$C_i = \dfrac{\partial g(x_{oi}, u_{oi})}{\partial x}$, and $D_i = \dfrac{\partial g(x_{oi}, u_{oi})}{\partial u}$.

Thus we get n linearized models P_i (i = 1, …, n) to approximate system (5) after gridding and linearization. Note that for every value of θ, there exists only one equilibrium point, which results in only one linearized model for every θ.

As is mentioned previously, when a nonlinear system is linearized about a series of equilibrium points, the gap metric and gap metric stability margin are applicable. Here, we will use them to define nonlinearity measures in the following subsections.

3.1. Nonlinearity measure based on gap metric and the maximum stability margin

Compute the gap-matrix [25] with all pairs of the n linearized models, and compute their maximum stability margins according to:

$$b_{opt}(P_i) = \sqrt{1 - \left\| \begin{bmatrix} \tilde{N}_i & \tilde{M}_i \end{bmatrix} \right\|_H^2} \tag{7}$$

where $P_i = \tilde{M}_i^{-1} \tilde{N}_i$ is the left normalized coprime factorization of P_i. Then we get an $n \times n$ matrix $gap = [\delta(P_i, P_j)]_{n\times n} := [\delta_{ij}]_{n\times n}$ and an $n \times 1$ vector $B_{opt} = [b_{opt}(P_i)]_{n\times 1} := [b_{opt}]_{n\times 1}$.

Among the n linearized models, choose the best local linear model P^* according to:

$$P^* := \left\{ P_m : \min_{1\le m\le n} (\max_{1\le i\le n} (\delta(P_m, P_i))) \right\} \tag{8}$$

Eq. (8) is called the mix-max principle, which means the biggest gap of the n gaps between P^* and the n linearized models is the smallest in the n linearized models. That is to say, in the n linearized models, P^* is the one that is the nearest to the n linearized models in the min-max sense. Therefore, P^* is the best local linear model.

The biggest gap $\delta_{\max}$ of the n gaps between P^* and the n linearized models is computed according to:

$$\delta_{\max}(P^*) = \max_{1\le i\le n} \delta(P^*, P_i) \tag{9}$$

Then the preliminary nonlinearity measure over the entire operating range is defined as:

$$NM_1 = \frac{\delta_{max}(P^*)}{b_{opt}(P^*)} \tag{10}$$

According to Proposition 1, if $NM_1 < 1$, there exists a linear controller that can theoretically stabilize nonlinear plant (5) in the whole operating space and the considered system is weakly nonlinear under the maximum stability criterion. Otherwise the considered system is strongly nonlinear, and it will be difficult or impossible to get a stabilizing linear controller for it over the entire operating range.

Because the maximum stability margin of the best local linear model P^* has nothing to do with the controller, therefore, NM_1 is a universal measure regardless of control strategies. It can be computed before a controller is designed, and supplies guidance for the controller design.

3.2. A CRNM based on gap metric and the actual stability margin

The **control-relevant nonlinearity measure** of system (5), *i.e.* NM_2 over the entire operating range is defined as:

$$NM_2 = \frac{\delta_{max}(P^*)}{b_{P^*,K}} \tag{11}$$

where K is a linear stabilizing controller designed based on P^*. From Proposition 1, we can get that system (5) under controller K is considered as closed-loop linear if $NM_2 < 1$ and K satisfies the desired performance requirements. Otherwise, if a linear controller with both $NM_2 < 1$ and acceptable performance cannot be acquired, then system (5) is not possible to be stabilized by the chosen control strategy, or a nonlinear control method is necessary. Quite a few linear control techniques can be used to design controllers, such as PID, MPC, LQ, and so on. In this work, H_∞ control method is employed to facilitate the comparison between the proposed method and the methods from Ref.[19] in the following sections.

NM_2 can be computed only after the linear controller is designed. It is used to judge whether the controller is enough for the considered system or not. It is dependent on both the system and the controller. Therefore, it is a **control-relevant nonlinearity measure.**

For both NM_1 and NM_2, the bigger the value is, the more nonlinear the system is. In the next subsection, the proposed nonlinearity measures are applied to two CSTR processes to demonstrate their use and effectiveness.

3.3. Case studies

3.3.1. Case 1. An isothermal CSTR (iCSTR)

Consider an iCSTR system with a first-order irreversible reaction, described by the following equation [26]:

$$\frac{dC_A}{dt} = -kC_A + (C_{Ai} - C_A)u \tag{12}$$

where C_A (mol/l) is the reactant concentration, u ($\min^{-1}$) is the input, C_{Ai} (1.0 mol/l) is the feed concentration, and k (0.028 $\min^{-1}$) is the rate constant.

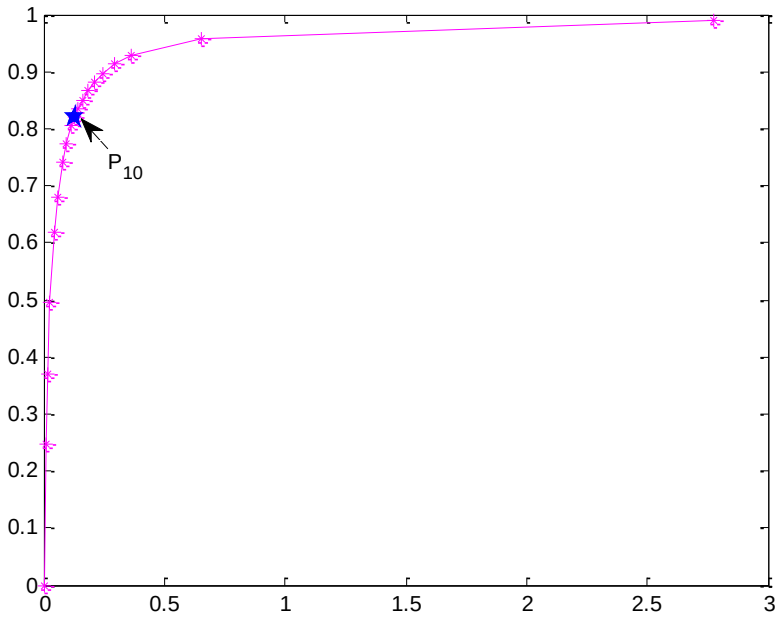

Fig.1. Static input-output curve of the iCSTR with 19 gridding points

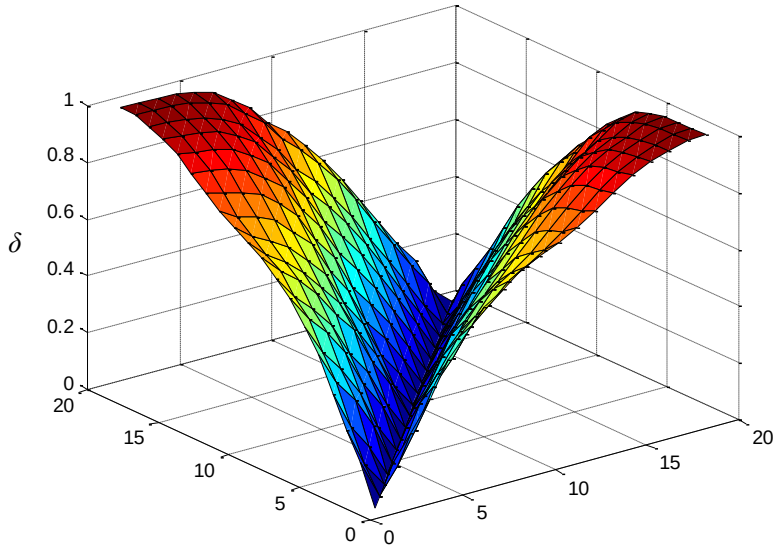

Fig. 2. Gaps between the 19 linearized models of the iCSTR

C_A is chosen as the scheduling variable of the iCSTR system for it captures the system's nonlinearity and the operating conditions. The operating space is $\{C_A \mid C_A \in [0,1]\}$. Applying the gap metric based dichotomy gridding algorithm [24] with γ_1 = 0.15 to the iCSTR, we get 19 gridding points, as shown in Fig. 1. The gaps between the 19 linearized models are displayed in Fig. 2. As is seen, the biggest gap is almost 1. The iCSTR has strong nonlinearity in the light of the open-loop nonlinearity measure based on gap metric [15]. Here the proposed control-relevant nonlinearity measures are used to measure the nonlinear degree of the iCSTR system.

For the 19 gridding points, the best local linear model is P_{10} based upon Eq.(8), as is marked in Fig. 1. And the biggest gap based on Eq.(9) is:

$$\delta_{max}(P_{10}) = 0.7551$$

The maximum stability margin of P_{10} is:

$$b_{opt}(P_{10}) = 0.9092$$

Therefore, the preliminary nonlinearity measure based on maximum stability margin is:

$$NM_1 = \frac{\delta_{max}(\mathrm{P}_{10})}{b_{opt}(\mathrm{P}_{10})} = \frac{0.7551}{0.9092} = 0.8305 < 1$$

Since $NM_1 < 1$, it means that there is a linear feedback controller that can stabilize the iCSTR over its whole operating space. So the system is not as nonlinear as the open-loop nonlinearity measure [15] indicates. Nevertheless, the nonlinearity measure based on maximum stability margin is an ideal measure. When the H_∞ control technique is used to design a local linear controller, we find it is hard to get a H_∞ controller based upon P_{10} with an acceptable closed-loop performance and $NM_1 < 1$. For a H_∞ controller based upon P_{10}:

$$NM_2 > 1$$

In the subsequent sections, the CRNM will be employed to decompose the iCSTR process into linear subsystems and design a multi-model H_∞ controller for set-point tracking and disturbance rejection control. Although a nonlinear, inverse model controller can be design for the iCSTR, the inverse control method needs an accurate nonlinear model [40]. Once there exist modeling errors, the control performance degrades. Besides, the inverse control method needs the

nonlinear dynamics to be invertible. It fails when the system exhibits input or output multiplicity, e.g. Case 2 in this work. Additionally, it may be computationally intensive to get a nonlinear dynamic inversion [40]. Therefore, the multi-model approach is employed here for its advantages mentioned previously.

3.3.2. Case 2: An exothermal CSTR (eCSTR)

Consider a benchmark eCSTR process in which an irreversible, first-order reaction takes place. The eCSTR process is modeled by [27]:

$$\begin{cases} \dot{x}_1 = -x_1 + D_a(1-x_1)\exp\left(\frac{x_2}{1+x_2/\gamma}\right) \\ \dot{x}_2 = -x_2 + BD_a(1-x_1)\exp\left(\frac{x_2}{1+x_2/\gamma}\right) + \beta(u-x_2) \\ y = x_2 \end{cases} \tag{13}$$

where the state variables x_1 and x_2 denote the dimensionless reagent conversion and reactor temperature, respectively. The input variable u represents the dimensionless coolant temperature. The constants in Eq. (13) are D_a = 0.072, γ = 20, B = 8 and β = 0.3, respectively. As shown in Fig. 3, the eCSTR process has strong output multiplicity. Since the output y captures the nonlinearity of the eCSTR plant, y is chosen as the scheduling variable. Then the operating space is $\{y \mid y \in [0,6]\}$.

The gap metric based gridding algorithm [24] is applied to the eCSTR process with γ_1 = 0.15, and we get 42 steady state points to grid its operating space $\{y \mid y \in [0,6]\}$, as shown in Fig. 4. Since the biggest gap is equal to 1, the system exhibits strong open-loop nonlinearity according to the gap metric based nonlinearity measure [15]. In the following, the proposed CRNM will be applied to the eCSTR process.

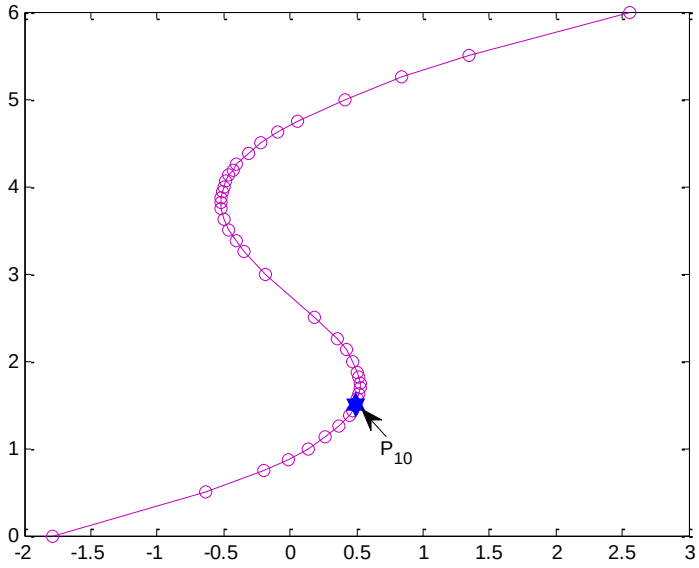

Fig. 3. Static input-output curve of the eCSTR with 42 gridding points

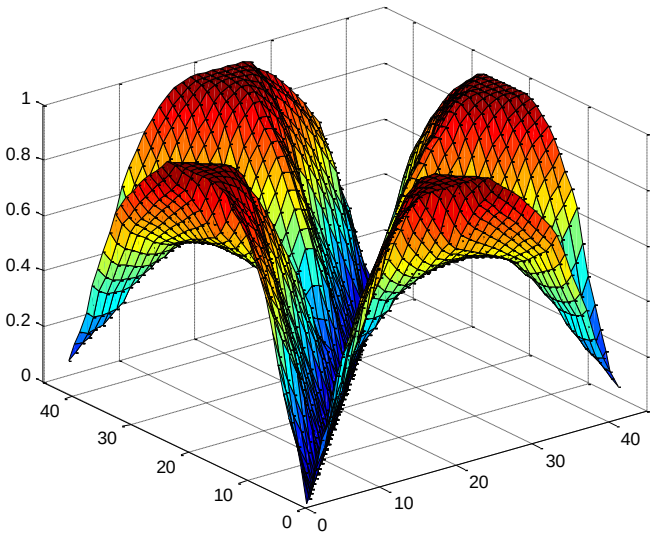

Fig. 4. Gap metrics between the 42 linearized models of the eCSTR.

For the 42 gridding points, the best local linear model is P_{10} based upon Eq.(8) as marked in Fig.3. And the biggest gap based upon Eq.(9) is:

$$\delta_{max}(P_{10}) = 0.7971$$

The maximum stability margin of P_{10} is:

$$b_{opt}(P_{10}) = 0.7861$$

Therefore, the preliminary nonlinearity measure based on maximum stability margin for the eCSTR process is:

$$NM_1 = \frac{\delta_{max}(P_{10})}{b_{opt}(P_{10})} = \frac{0.7971}{0.7861} = 1.014 > 1$$

Since $NM_1 > 1$, it is difficult to get a linear controller to stabilize the eCSTR process in the whole operating space, and $NM_2 > 1$ for any H_∞ controller. In the following, the CRNM will be used to propose an integrated multi-model control approach for both set-point tracking control and disturbance rejection control.

Note that although the best local linear model of the eCSTR is also P_{10} just like the iCSTR, the two P_{10} models are totally different. There is no relation between the two models. For example, if $\gamma_1 = 0.13$ is used to grid the eCSTR, we will find the best local linear model is P_{11} which is also at the point marked by blue hexagram in Fig. 3. In order to make a clear and direct comparison with the method in Ref.[19] in the following sections, we continue to use $\gamma_1 = 0.15$ in this work as in Ref. [19].

4. A CRNM-based integrated multi-model control framework

In this work, we are to propose a CRNM-based integrated multi-model control framework, which makes full use of the advantages of the two algorithms from Ref. [19], while avoiding their disadvantages. It means that given a control strategy for local linear controller design, an appropriate linear model bank for multi-model controller design is acquired systematically with less computational load and without model redundancy while the local controllers are designed. Namely, the local model selection is closely integrated with the local controller design. Moreover, the local stability of the system in every subregion is guaranteed by the corresponding local controller. Like most multi-model control approaches for nonlinear systems, the global stability of

the nonlinear system cannot be guaranteed. As in Ref. [19], many linear control techniques, such as H_∞, PID, IMC, LQ, and so on, can be used in the proposed multi-model control framework and H_∞ control algorithm is continued to be employed to design local controllers to make the comparisons in the following sections simple and clear. Moreover, a $1/\delta$ gap-based weighting algorithm, which is simple, easy and effective to apply, is formulated to combine the local controllers.

The proposed CRNM-based integrated multi-model control approach which includes a CRNM-based multi-model decomposition and local controller design algorithm and a gap-based weighting algorithm, is detailed as follows.

4.1. CRNM-based multi-model decomposition and local controller design

For the nonlinear system (5), the procedure of the CRNM-based multi-model decomposition and local controller design is summarized as the following algorithm.

4.1.1. Algorithm

Step1: Grid the operating space of system (5) through the gap metric based dichotomy gridding algorithm [24] and linearize system (5) about the gridding points. Suppose we get n linearized models P_i (i = 1, …, n).

Step2: Compute the gap-matrix [25] between all pairs of the n linearized models, and get their maximum stability margins according to Eq. (7). Then we get an $n \times n$ matrix $gap = [\delta(P_i, P_j)]_{n\times n} := [\delta_{ij}]_{n\times n}$ and an $n \times 1$ vector $B_{opt} = [b_{opt}(P_i)]_{n\times 1} := [b_{opt}]_{n\times 1}$.

Step3: Set k = 1, and N_m = 0.

Step4: If k <= n, set l = k and $N_m = N_m + 1$. Otherwise, go to Step12.

Step5: Choose the best local linear model P^* among the kth to lth linearized model according to:

$$P^* := \left\{ P_m : \min_{k\le m\le l} (\max_{k\le i\le l} (\delta(P_m, P_i))) \right\} \tag{14}$$

Step6: Compute the biggest gap $\delta_{\max}$ between P^* and the other linearized models according to:

$$\delta_{\max} = \max_{k\le i\le l} \delta(P^*, P_i) \tag{15}$$

Step7: If $NM_1 = \delta_{max}(P^*)/b_{opt}(P^*) < 1$, set $l = l + 1$ and return to Step5; otherwise, go to Step8.

Step8: Set $l = l - 1$.

Step9: Design a linear controller K for the best linear model P^*. If K satisfies both $NM_2 = \delta_{max}(P^*)/b_{P,k}(P^*) < 1$ and the desired performance requirements, then the $l - k + 1$ successive linearized models are classified into one subregion, represented by their local linear model P^* and stabilized by the corresponding controller K. Set $k = l + 1$, and go back to Step4.

Step10: If an acceptable controller K with $NM_2 = \delta_{max}(P^*)/b_{P,k}(P^*) < 1$ is not found, Set $l = l - 1$.

Step11: Re-select P^* among the kth to lth linearized model according to $P^* := \left\{ P_m : \min_{k\le m\le l} (\max_{k\le i\le l} (\delta(P_m, P_i))) \right\}$, and re-compute the biggest gap $\delta_{\max}(P^*)$ between P^* and the other linearized models. Go back to Step 9.

Step12: The n linearized models are divided into N_m subregions with N_m local models and N_m linear controllers.

Finally, the process (5) is decomposed into N_m local models with N_m local linear controllers

which will be combined into a multi-mdoel controller by a $1/\delta$ gap-based weighting method in the subsequent sections.

Remark 1: N_m is the number of the subregions, *i.e.*, the number of local linear models and local controllers.

Remark 2: In Step9, the $l - k + 1$ successive linearized models are classified into one subregion and represented by P^* according to the NM_1 criterion.

Remark 3: In the above procedure, NM_1 is used to perform the preliminary decomposition; NM_2 is used to perform the final decomposition. The use of NM_1 reduces the computational load greatly; and the use of NM_2 makes the decomposition more effective and less dependent on previous knowledge. Therefore, the above procedure combines the strong points of Algorithm 1 & Algorithm 2 in Ref. [19].

Remark 4: Just as in Ref. [19], the local model determination and local controller design are carried out sequentially, making the two steps closely connected with each other. Also, the above design procedures are somewhat conservative as a result of the conservativeness of Proposition 1. Local controllers which do not satisfy the CRNM criteria may have better performance.

4.1.2. Case study

In the following, the proposed Algorithm is applied to the above two CSTR processes.

Case 1: The iCSTR

Here, we will apply the proposed CRNM-based multi-model decomposition and local controller design procedure to the iCSTR process. The detailed procedure is listed step by step as follows.

S1. For the 19 gridding points, we divide the system preliminarily according to the maximum stability margin based NM_1, getting the result shown in Table 1.

Table 1. Preliminary decomposition for 1st subregion of iCSTR

Subregion	Operating point	NM_1
1→19	10th	$NM_1 = \delta_{\max}(P_{10})/b_{opt}(P_{10}) = 0.7551/0.9092 < 1$

S2: On the basis of S1, perform the final decomposition according to the actual stability margin based NM_2, and get the result in Table 2.

Table 2. Final decomposition for 1st subregion of iCSTR

Subregion	Operating point	NM_2
1→15	8th	$NM_2 = \delta_{\max(P_8)}/b_{pk}(P_8) = 0.6527/0.7024 < 1$

S3: For gridding points 16→19, carry out the preliminary decomposition and get Table 3.

Table 3. Preliminary decomposition for 2nd subregion of iCSTR

Subregion	Operating point	NM_1
16→19	17th	$NM_1 = \delta_{\max(P_{17})}/b_{opt}(P_{17}) = 0.1785/0.9958 < 1$

S4: On the basis of S3, perform the final decomposition and get Table 4.

Table 4. Final decomposition for 2nd subregion of iCSTR

Subregion	Operating point	NM_2
16→19	17th	$NM_2 = \delta_{\max(P_{17})}/b_{pk}(P_{17}) = 0.1785/0.1821 < 1$

The final decomposition result of the iCSTR process is summarized in Table 5.

Table 5. CRNM-based multi-model decomposition and local controllers of the iCSTR

Subregion	1st	2nd
Linearized models included	1→15	16→19
Operating point of the local	8th	17th
linear model (C_A, u)	(0.7734,0.0956)	(0.9281,0.3616)
Local linear model	$P_1^* = \frac{0.2266}{s+0.1236}$	$P_2^* = \frac{0.07188}{s+0.3896}$
subrange	$0 \le C_A \le 0.9$	$0.9 < C_A \le 1$
Local linear controller	$K_1 = \frac{9.541s+1.179}{s^2+11.27s+0.009389}$	$K_2 = \frac{2.695s+1.05}{s^2+0.8866s+0.0007381}$
NM_2	0.6527/0.7024<1	0.1785/0.1821<1

From Table 5, we can see that the system is divided into 2 subregions. The 1st subregion contains 15 linearized models (1→15), and the local linear model for the 1st subregion is the 8th linearized model $P_1^* = 0.2266/(s+0.1236)$, with operating point ($C_A$, u) = (0.7734, 0.0956). The first subrange is $\{C_A | 0 \le C_A \le 0.9\}$. The local linear H_∞ controller $K_1 = \frac{9.541s+1.179}{s^2+11.27s+0.009389}$ with $NM_2 < 1$ is designed. The other column is interpreted in the same way. Note that K_1 does not have an explicit integral action, but it has a pole − 0.0008, which is near the origin. Therefore, K_1 has an approximate integral action, making it proper for tracking control of step changes for the iCSTR process. So is K_2.

The above decomposition result is ***the same as*** in Ref. [19]. Namely, the proposed CRNM-based multi-model decomposition method is as effective as the algorithms from Ref. [19] in avoiding model redundancy. However, the computational load is much less. Since there is a tuning parameter ε, Algorithm 2 in Ref. [19] is not as systematical as Algorithm 1 in Ref. [19]. In the following we therefore only compare the computational load between the proposed method and Algorithm 1 in Ref. [19].

Using the proposed algorithm in this work, for the 1st subregion, 5 H_∞ controllers are designed and tested, and for the 2nd subregion, 1 H_∞ controller is designed and tested. In total, 6 H_∞ controllers are designed and tested.

However, in Ref. [19], 14 H_∞ controllers are designed and tested for the 1st subregion, and 3 H_∞ controllers for the 2nd subregion. In total, 17 H_∞ controllers.

The number of controllers that are designed and tested is denoted as “repeat times” for simplicity in the following. Table 6 shows the computational load of the proposed method and Algorithm 1 from Ref. [19].

Table 6. Comparison between the CRNM-based method and Algorithm 1 from Ref. [19].

Repeat times	CRNM-based method	Algorithm 1 from Ref. [19]
1st subregion	5	14
2nd subregion	1	3
Total	6	17

Therefore, the computational load of Algorithm 1 from Ref. [19] is almost three times of the proposed algorithm for the iCSTR process. So the proposed algorithm reduced computational load

greatly.

Case 2: The eCSTR

As we know from Section 3, the control-relevant nonlinearity measure of the eCSTR process is strong since $NM_1 > 1$. It is quite difficult to design a single linear controller to stabilize the eCSTR process over the whole operating range. Therefore, the CRNM-based method is applied to it to get a multi-model controller.

The detailed decomposition of the eCSTR system is listed as follows:

S1: Perform the preliminary decomposition of the 42 gridding points according to the maximum stability margin based NM_1, and get the following decomposition result in Table 7.

Table 7. Preliminary decomposition for 1st subregion

Subregion	Operating point	NM_1
1→19	9th	$NM_1 = \delta_{max}(P_9)/b_{opt}(P_9) = 0.7922/0.8137 < 1$

S2: On the basis of S1, perform the final decomposition of the 1st subregion according to the actual stability margin based NM_2, and get the result in Table 8.

Table 8. Final decomposition for 1st subregion

Subregion	Operating point	NM_1
1→16	8th	$NM_2 = \delta_{max}(P_8)/b_{pk}(P_8) = 0.6780/0.6797 < 1$

S3: Perform the preliminary decomposition of the 2nd subregion according to the maximum stability margin based NM_1, and get Table 9.

Table 9. Preliminary decomposition for 2nd subregion

Subregion	Operating point	NM_1
17→30	25th	$NM_1 = \delta_{max}(P_{25})/b_{opt}(P_{25}) = 0.4332/0.4786 < 1$

S4: Perform the final decomposition of the 2nd subregion according to the actual stability margin based NM_2, and we get the result as follows in Table 10.

Table 10. Final decomposition for 2nd subregion

Subregion	Operating point	NM_1
17→30	25th	$NM_2 = \delta_{max}(P_{25})/b_{pk}(P_{25}) = 0.4332/0.4432 < 1$

S5: Perform the preliminary decomposition of the 3rd subregion according to the maximum stability margin based NM_1, and get Table 11.

Table 11. Preliminary decomposition for 3rd subregion

Subregion	Operating point	NM_1
31→42	36th	$NM_1 = \delta_{max}(P_{36})/b_{opt}(P_{36}) = 0.5249/0.8471 < 1$

S6: Perform the final decomposition of the 3rd subregion according to the actual stability margin based NM_2, and we get the result as follows in Table 12.

Table 12. Final decomposition for 3rd subregion

Subregion	Operating point	NM_1
31→42	36th	$NM_1 = \delta_{max}(P_{36})/b_{pk}(P_{36}) = 0.5249/0.5326 < 1$

The decomposition of the eCSTR process is completed. The local models and controllers are

summarized in Table 13.

Table 13. CRNM-based multi-model decomposition and local controllers of the eCSTR

Subregion	1st	2nd	3rd
Linearized model included	1→16	17→30	31→42
Operating point of local linear model (x_1, x_2, u)	8th (0.2068,1.375, 0.4446)	25th (0.6077,3.625, -0.4937)	36th (0.7393,4.5,-0.2149)
Local linear model	$P_1^* = \frac{0.3s+0.3782}{s^2+1.113s+0.191}$	$P_2^* = \frac{0.3s+0.7647}{s^2+0.3649s-0.170}$	$P_3^* = \frac{0.3s+1.151}{s^2+1.195s+1.045}$
subrange	$0 \le y \le 2$	$2 < y \le 4$	$4 < y \le 6$
Local linear controller	$K_1 = \frac{40.82s^2+45.44s+7.785}{s^3+43.9s^2+43.27s+0.0075}$	$K_2 = \frac{32.53s^3+47.68s^2+17.99s+0.528}{s^4+19.14s^3+39.44s^2+20.58s+0.619}$	$K_3 = \frac{167.7s^2+200.5s+175.3}{s^3+107.4s^2+161.7s+0.162}$
NM_2	0.6780/0.6797<1	0.4332/0.4432<1	0.5249/0.5326<1

Table 13 can be interpreted similarly as Table 5. As displayed in Table 13, the eCSTR is approximated by 3 local models with no integral elements, and 3 local H_∞ controllers are designed using the CRNM-based integrated multi-model control approach. As to the 3 H_∞ controllers in Table 13, we can also find that they have approximate integral actions, and therefore there are appropriate for tracking control of step changes, too.

Evidently, the decomposition result is the same as in Ref. [19], which validates that the proposed CRNM-based multi-model control method is as effective as the methods from Ref. [19] in selecting local models and designing local controllers. Next, we will compare the computational load.

Using the proposed method in this work, repeat times are 4 for the first subregion, 1 for the 2nd subregion, and 1 for the 3rd subregion. In total 6 H_∞ controllers are designed and tested. However, in Algorithm 1 of Ref. [19], repeat times are 15 for the 1st subregion, 13 for the 2nd subregion, and 11 for the 3rd subregion. 39 H_∞ controllers are designed and tested in total, more than 6 times of that using the proposed method as shown in Table 14. Therefore, the proposed CRNM-based decomposition and local controller design method is much more efficient.

Table 14 Comparison between the CRNM-based method and Algorithm 1 from Ref. [19].

Repeat times	CRNM-based method	Algorithm 1 in Ref. [19]
1st subregion	4	15
2nd subregion	1	13
3rd subregion	1	11
Total	6	39

In summary, the proposed CRNM-based method can get the same decomposition result as the algorithms in Ref. [19]. Nevertheless, distinct from Algorithm 1 in Ref. [19], the proposed method reduces computation largely, so it is more efficient; different from Algorithm 2 in Ref. [19], the proposed method is independent of a prior knowledge, so it is more systematical. In short, the proposed method combines the advantages while avoids the disadvantages.

In the next section, a $1/\delta$ gap-based weighing method is proposed to combine the local controller into a global multi-model controller, which is also according to the gap metric criterion.

4.2. A weighting method based on gap metric

For the nonlinear system described by Eq. (5), at time t, the value of θ is denoted as θ_t. The steady state point corresponding to θ_t is denoted by (x_{ot}, u_{ot}, y_{ot}). Then the linearized model

obtained by linearizing system (5) around (x_{ot}, u_{ot}, y_{ot}) is denoted as $P(\theta_t)$:

$$\begin{cases} \delta\dot{x} = A_t \delta x + B_t \delta u \\ \delta y = C_t \delta x + D_t \delta u \end{cases} \tag{16}$$

where $\delta x = \delta x - x_{ot}$, $\delta u = \delta u - u_{ot}$, $\delta y = \delta y - y_{ot}$, $A_{ot} = \frac{\partial f(x_{ot}, u_{ot})}{\partial x}$, $B_{ot} = \frac{\partial f(x_{ot}, u_{ot})}{\partial u}$, $C_{ot} = \frac{\partial g(x_{ot}, u_{ot})}{\partial x}$, and $D_{ot} = \frac{\partial g(x_{ot}, u_{ot})}{\partial u}$.

4.2.1. 1/δ weighting method

At time t, nonlinear system (5) is denoted as nP_t. Then $P(\theta_t)$ is the linearized model of nP_t. The gap metric between nP_t and the local linear system P_i is defined as the gap metric between $P(\theta_t)$ and P_i, denoted as $\gamma_i(\theta_t)$:

$$\gamma_i(\theta_t) = \delta(P_i, P(\theta_t)), \; i = 1, \ldots, N_m \tag{17}$$

Then the weighting function of the ith local linear controller at time t is established as:

$$\varphi_i(\theta_t) = \frac{\left(\frac{1}{\gamma_i(\theta_t)}\right)^{k_w}}{\sum_{j=1}^{N_m}\left(\frac{1}{\gamma_j(\theta_t)}\right)^{k_w}} \qquad i = 1, \ldots, N_m \tag{18}$$

where $k_w \geq 1$ is a tuning parameter. φ_i satisfies $\sum_{i=1}^{N_m} \varphi_i(\theta_t) = 1$.

Therefore, the output of the multi-model controller is:

$$u(t) = \sum_{i=1}^{N_m} \varphi_i(\theta_t) u_i(t) \tag{19}$$

where $u_i(t)$ is the ith local linear controller's output. According to Eq. (18), a bigger gap will lead to a smaller weight, and vice versa. The weighting method formed by Eqs.(17)-(18) is called 1/δ weighting method for simplicity.

For nonlinear system (5), suppose we get three local linear models (P_1, P_2, P_3) by the proposed CRNM-based Algorithm. Then Fig. 5 shows a graphic interpretation of the 1/δ weighting method along the system's transition and static locus. At time instant t, the gaps between the nonlinear system nP_t and local linear model P_i (i = 1, 2, 3) are denoted by γ_i (i = 1, 2, 3). According to the implication of the gap metric, a big γ_i indicates that the dynamic behavior of P_i is far apart from the nonlinear system's. Therefore, the corresponding controller has a small φ_i and plays a minor role in the multi-model controller, and vice versa. Apparently, the 1/δ weighting method is more intuitive compared to Gaussian and Trapezoidal functions.

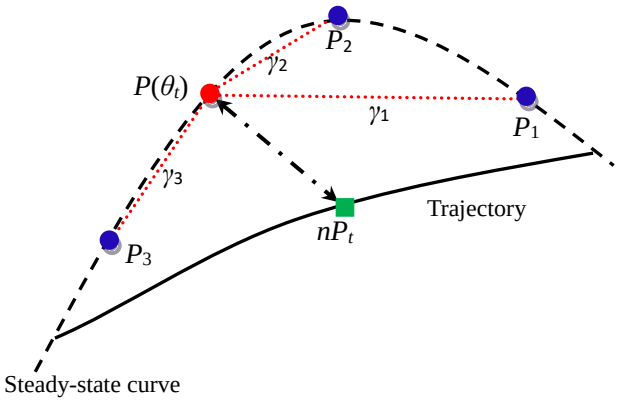

Fig. 5. Illustration of the 1/δ weighting method

Like the 1-δ weighting method from Ref. [20], (a) the proposed weighting functions can be

computed off-line and saved as look-up tables since Eqs.(17)-(18) are only dependent on θ but independent of t. Therefore, online computational load is reduced and the method is more efficient. (b) There exists merely one tuning parameter in the $1/\delta$ gap-based method regardless of the number of scheduling variables, whereas the number of parameters for traditional weighting methods, e.g. Gaussian and Trapezoidal functions, relies on the number of scheduling variables heavily. Hence the proposed $1/\delta$ gap-based method is comparatively much simpler.

Compared to the weighting method in Ref. [20], the proposed weighting method in this work is more sensitive to its tuning parameter k_w, making it easier to get a proper weight for a local controller. We will discuss this in the following.

4.2.2. Case studies-comparison between two gap-metric-based weighting methods

In the section, we will show the difference between the 1-δ and $1/\delta$ gap-metric-based methods by the CSTR processes.

Based on the decomposition results of the two CSTR systems in Section 4.1, we can get the look-up tables of weights easily. For weights that cannot be found in the tables directly, linear interpolation is used in this work. Figures of weights will be shown instead of look-up tables for intuitiveness in the following.

4.2.2.1. The iCSTR

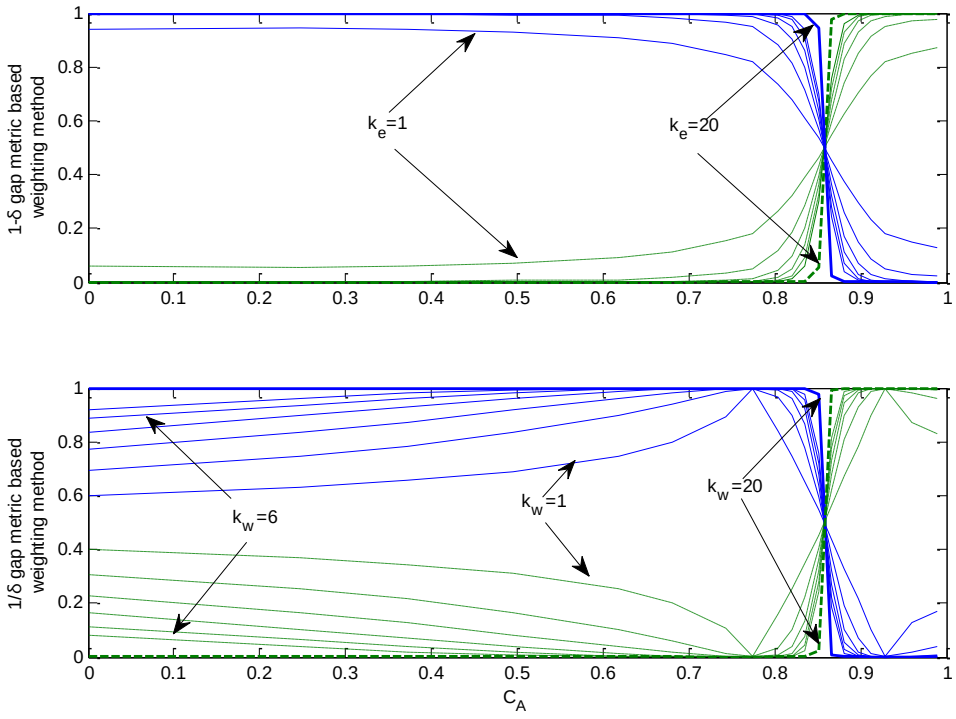

Fig. 6. Weights of two gap-metric-based weighting methods for iCSTR (Solid—weights for the 1st controller, dash—weights for the 2nd controller)

For the iCSTR, we will make a comparison between the proposed $1/\delta$ weighting method and the 1-δ weighting method in this section.

Fig. 6 shows a set of weighting functions with different values of tuning parameters (k_e and k_w grow from 1 to 20). The upper subplot gives the 1-δ weights of the two local controllers with different values of k_e. The lower subplot depicts the 1/δ weights of the two local controllers with different values of k_w. The solid lines are weights for the 1st local controllers, and the dash lines

are for the 2nd local controllers. It is clearly seen that (1)When k_e and k_w grow bigger and bigger, the two weighting methods will have the similar weights for each local controller. (2)The variation ranges of the proposed 1/δ weights are wider than the 1-δ weights. (3)The proposed 1/δ weighting method is more sensitive to the variation of k_w, while the 1-δ method is less sensitive when k_e changes. (4)The proposed 1/δ weights have peaks equal to 1 in their subregions for smaller k_w. The peaks are located at the operating points of local linear models. The *i*th local controller should have a weight equal to 1 when the system transits to the *i*th operating point. It is reasonable that each curve of the weights should at least have a value equal to 1 regardless of the value of the tuning parameters. Therefore, the 1/δ weights are more intuitive than the 1-δ weights.

4.2.2.2. The eCSTR

Fig. 7 displays a set of weights for the three local controllers of the eCSTR system when k_e and k_w grow from 1 to 50. The upper subplot shows the 1-δ weights of the three local controllers with different values of k_e. The lower subplot shows the 1/δ weights of the three local controllers with different values of k_w. The solid lines are weights for the 1st local controller, the dash lines are for the 2nd local controller, and the dotted lines are for the 3rd local controller. Obviously, the 1/δ weights have a wider range in its own subregion than 1-δ weights; 1/δ weights have peaks while 1-δ weights are smoother; the1/δ weights have peak values equal to 1, while the 1-δ weights have peak smaller than 1. In summary, the 1/δ weights are more flexible and sensitive to the tuning parameter in their own subregions. Namely, the two weighting methods have the similar features as in the iCSTR.

From the above experiments, we can get the conclusion that, the proposed 1/δ weighting method is more sensitive to the tuning parameter, which makes it easier to get a proper weight for a local controller.

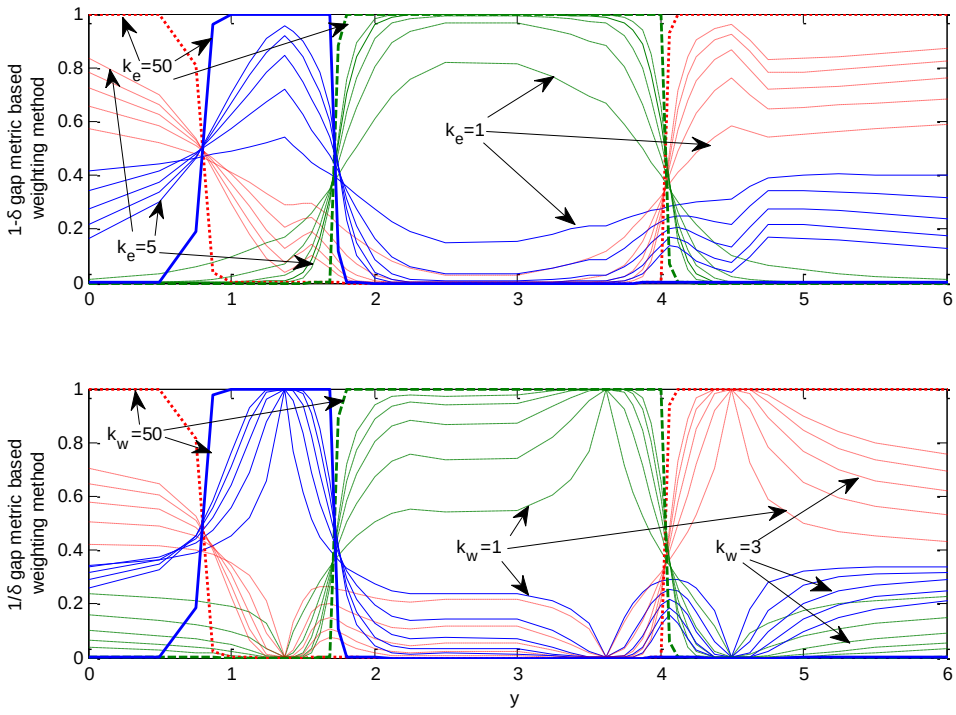

Fig. 7. Weights of two gap-metric-based weighting methods for eCSTR (Solid—weights for the 1st controller, dash—weights for the 2nd controller, dot—weights for the 3rd controller)

5. Closed-loop simulations

In this section, closed-loop simulations of set-point tracking and disturbance rejection control are displayed for the above two CSTR processes to demonstrate the effectiveness of the proposed CRNM-based integrated multi-model control approach. For comparison, the 1-δ weighting method and trapezoidal weighting method from literature are also used to combine multi-model H_∞ controllers.

5.1. Case1: The iCSTR

The proposed 1/δ gap-metric-based weighting functions with k_w = 6 shown in Fig. 6 are used for the iCSTR. For comparison, the 1-δ gap-based weighting functions with k_e = 1 shown in Fig. 6 and trapezoidal functions shown in Fig. 8 are also employed to get multi-model H_∞ controllers. Parameters of the trapezoidal and 1-δ weighting functions are well tuned. Then the two local H_∞ controllers from Table 5 are combined into three multi-model H_∞ controllers. Note that for the iCSTR system, there is only one tuning parameter in every gap-based weighting method, while there are 4 tuning parameters in the trapezoidal weighting method.

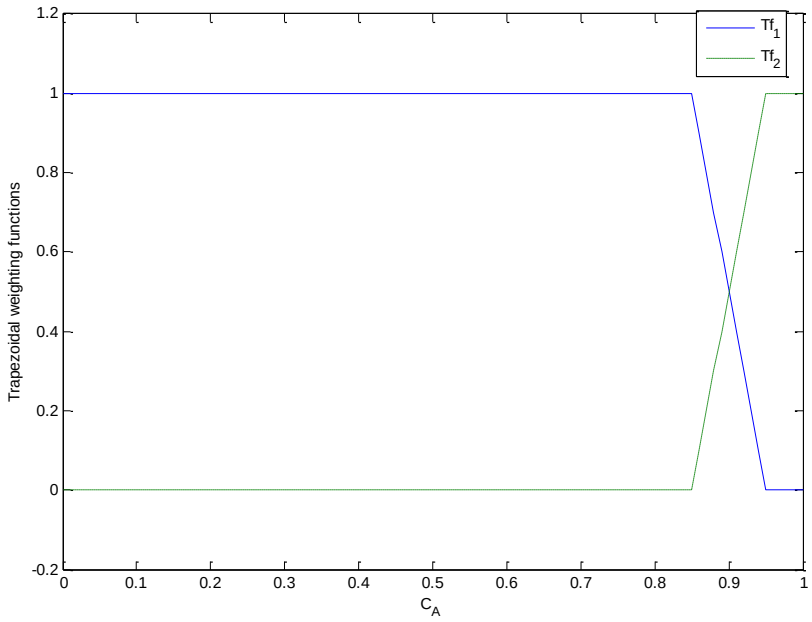

Fig. 8. Trapezoidal weighting functions for the iCSTR system (with 4 tuning parameters)

Closed-loop responses of the iCSTR process using three multi-model H_∞ controllers are displayed in Figs. 9 and 10. The one using the 1/δ gap-based weighting method has C_{Ag} as its output and u_g as its input; the one using the trapezoidal weighting functions has its output C_{AT} and input u_T; and the one using the 1-δ weighting method has C_{A0} and u_0.

On the whole, the three multi-model controllers have similar performances for set-point tracking control as shown in Fig. 9. All outputs track the reference signals fast and accurately without big overshoots or big static errors, and all the inputs vary in the feasible range. Transitions between the two subregions are also satisfactory: fast, smooth, and no chattering. In order to make a closer comparison among the three multi-model controllers and the three weighting methods, we calculate the integrated absolute error (IAE) values: $IAE_g = 92.1538 < IAE_0 = 92.3390 < IAE_T = 95.8575$. Thus, the proposed 1/$\delta$ gap-based multi-model H_∞ controller is slightly better than the one using the 1-δ gap-based weighting method, and better than the one using the trapezoidal

weighting method.

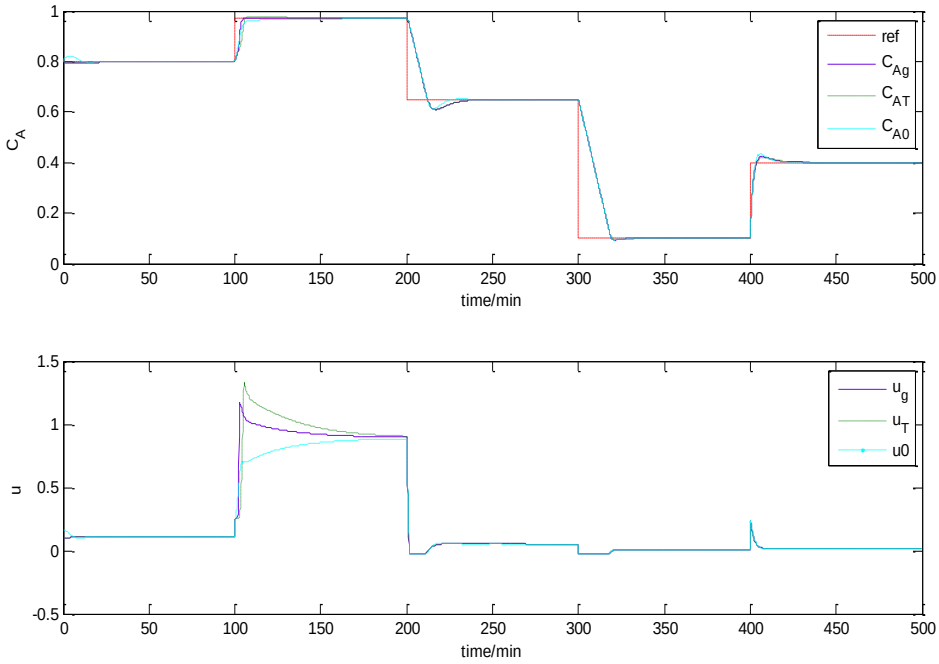

Fig. 9. Set-point tracking control of the iCSTR

Disturbance rejection control responses of the iCSTR process using the three multi-model H_∞ controllers are displayed in Fig. 10. When the process is in subregion 2, a disturbance $v_1 = 0.03$ enters the output at *time* = 90, and leaves at *time* = 180. During the stay in subregion 1, another disturbance $v_2 = 0.1$ appears at *time* = 350 and disappears at *time* = 430. In both cases, C_{Ag} and C_{A0} return to the reference signal promptly and accurately whenever the disturbance occurs or goes away. However, C_{AT} is a bit oscillatory when v_1 appears, making $IAE_T = 55.0693$ significantly bigger than the other two: $IAE_g = 52.2502$ and $IAE_0 = 52.9516$. The proposed $1/\delta$ based multi-model controller is slightly better than the $1\text{-}\delta$ based multi-model controller since $IAE_g < IAE_0$, although both the gap-metric-based multi-model controllers have good disturbance rejection control performances: both react to the disturbances immediately and bring back C_A to the reference signal rapidly and accurately.

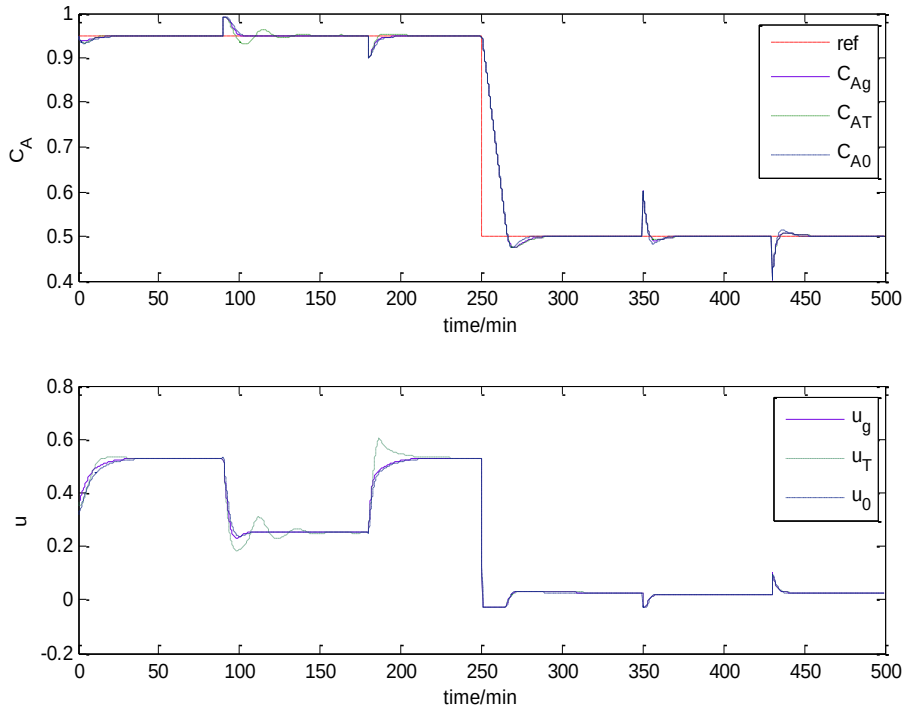

Fig. 10. Disturbance rejection control of the iCSTR

From the closed-loop responses of the iCSTR system, we can see that the proposed multi-model controller has a better performance than the other two for both set-point tracking and disturbance rejection control. Therefore, the CRNM-based integrated multi-model control design method is effective in selecting local models, designing local controllers, and scheduling local controllers.

5.2. Case 2 : The eCSTR

For the eCSTR process, the 1/δ gap-based weighting functions with k_e=3 shown in Fig. 7 are used to combine the 3 local H_∞ controllers from Table 13 to get a global multi-model H_∞ controller. For comparison, the 1-δ gap-based weighting functions and trapezoidal functions shown in Figs. 7 and 11 are also used to combine the three local H_∞ controllers from Table 13. Closed-loop responses are shown in Figs. 12-13. The output of the 1/δ gap-based closed-loop system is y_g with the control input u_g, the output of the 1-δ gap-based system is y_0 with its input u_0, while the output of the other system is y_T with its input u_T.

Note that for the eCSTR systems, there exists merely one tuning parameter in each of the gap-based weighting methods, while in the trapezoidal functions shown in Fig. 11, there are 8 tuning parameters.

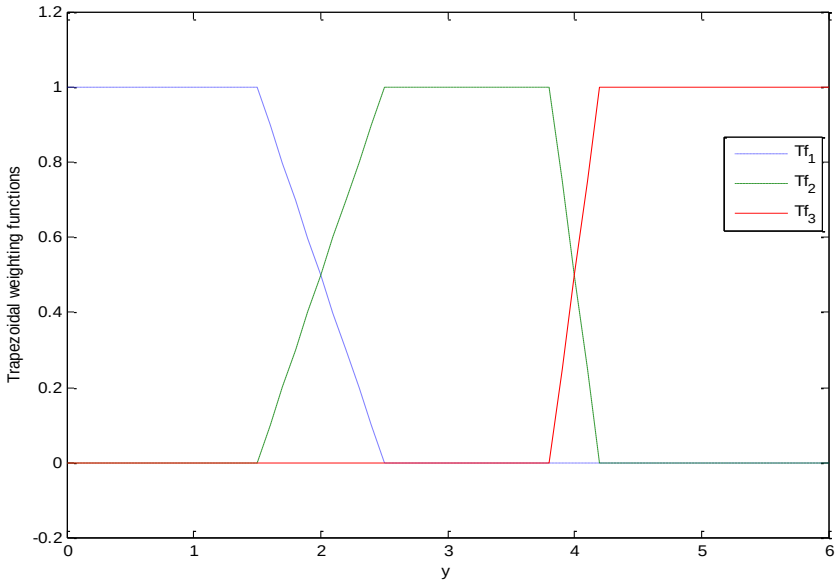

Fig.11. Trapezoidal weighting functions for the eCSTR with 8 tuning parameters

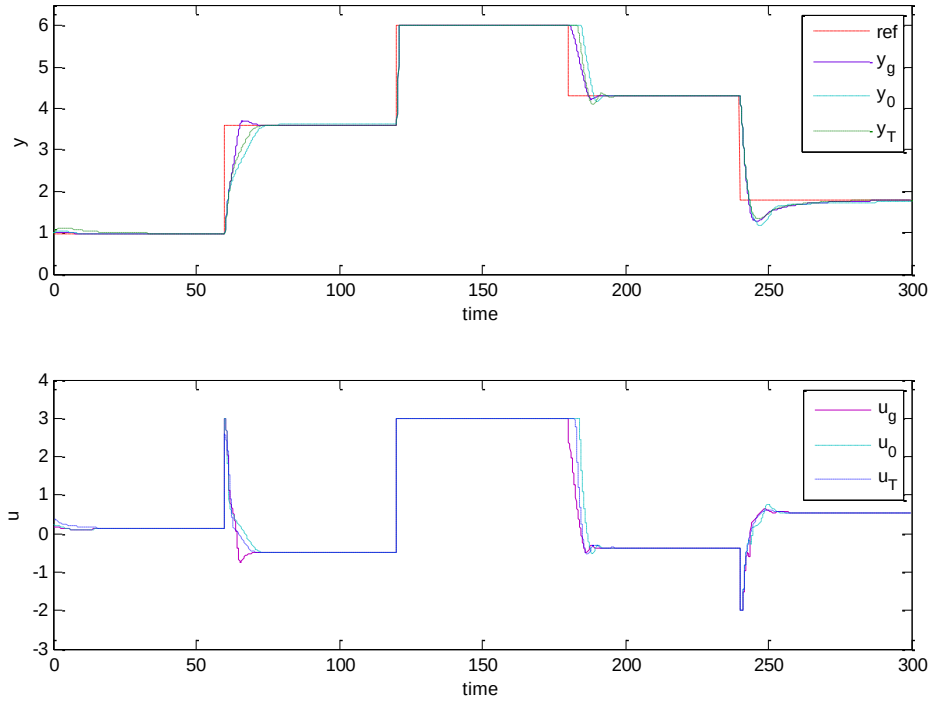

Fig. 12. Set-point tracking control of the eCSTR

Fig. 12 shows the set-point tracking control of the three multi-model H_∞ controllers for the eCSTR process. Obviously, all the three outputs follow the reference signal closely as a whole, but y_g is faster than the other two. The IAE values are IAE_g = 262.3101, IAE_T = 321.8751, and IAE_0 = 372.9597(k_e = 5), respectively. Apparently, $IAE_g < IAE_T < IAE_0$. Therefore, the 1/δ gap metric based multi-model controller has the best performance among the three controllers, and the trapezoidal functions based multi-model controller performs better than the 1-δ based multi-model

controller for the eCSTR in set-point tracking control regarding to the IAE criterion. Note that the gap-based weighting methods have much fewer tuning parameters, making them easier to use.

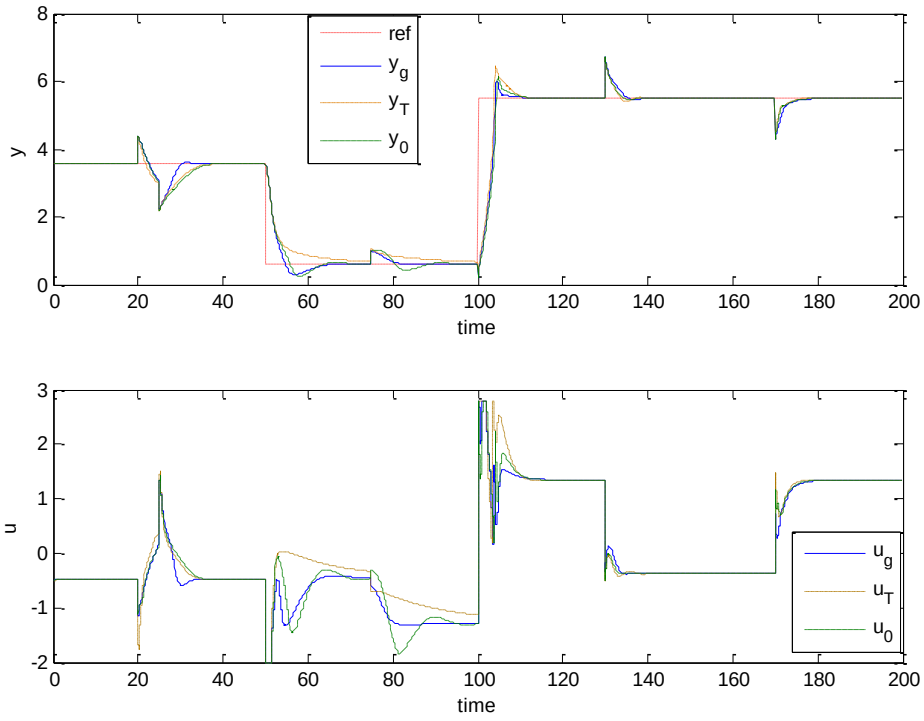

Fig.13. Disturbance rejection control of the eCSTR

When it comes to disturbance rejection control, the proposed multi-model H_∞ controller based on CRNM performs better than the other two as shown in Fig. 13. Obviously, y_g is faster and more accurate in each subregion than y_0 and y_T. Especially, in the 1st subregion during *time* = 50 to 100, there is a big static error for y_T. Besides, y_T has a bigger overshoot when the setpoint changes to the 3rd subregion. The proposed controller can reject disturbance effectively and bring the output back to the setpoint quickly, while the other two multi-model H_∞ controllers perform relatively not so well. The IAE values are IAE_g = 339.2100, IAE_T = 418.9340, IAE_0 = 397.1170, respectively.

From the simulation results of the two CSTR systems, it is concluded that:

1) The CRNM-based multi-model decomposition and local control design method is as effective as the algorithms in Ref. [19], but more efficient and systematic. So linear model redundancy is largely avoided, computational load is greatly reduced, and dependency on a prior knowledge is reduced.
2) The proposed $1/\delta$ weighting method is simple and effective. The resulting multi-model controller can have a performance as good as or even better than traditional weighting methods with less tuning effort.
3) Compared with the $1\text{-}\delta$ weighting method, the $1/\delta$ method is consistently good, but the $1\text{-}\delta$ method is sometimes not as good as traditional methods.

6. Conclusions

A gap-based CRNM method is proposed for quantification of the nonlinearity degree of a process when a linear control strategy is chosen. If the nonlinearity measures are larger than 1, a

nonlinear control algorithm may be needed. Otherwise, the designed linear controller is capable to stabilize the process over the whole operating space. Supported by the control-relevant nonlinearity measures, an integrated multi-model control framework is proposed. A bank of local models and controllers can be selected and designed systematically with little previous knowledge, with small computational cost, and without model redundancy. A $1/\delta$ gap-based weighting method is developed for local controller combination. Two CSTR chemical processes are studied and comparisons have been made among the proposed approaches and other typical methods. It is demonstrated by the closed-loop simulations that the CRNM-based integrated multi-model control approach can get an effective model/controller bank, and schedule the local controllers more effectively.

Acknowledgments

This work is supported by the NSF of China (61104079), NSF of Jiangsu Province (BK20150854), and by the Fundamental Research Funds for the Central Universities (2016B15414).

References

[1] M. Guay, P.J. McLellan, D.W. Bacon, Measurement of nonlinearity in Chemical Process Control Systems: The Steady State Map, The Canadian Journal of Chemical Engineering 73 (1995) 868-882.

[2] T. Schweickhardt, F. Allgower, Linear control of nonlinear systems based on nonlinearity measures, Journal of Process Control 17 (2007) 273-28.

[3] M. Nikolaou, P. Misra, Linear control of nonlinear process: recent developments and future directions, Computers and Chemical Engineering 27 (2003) 1043-1059.

[4] A. Helbig, W. Marquardt, F. Allgower, Nonlinearity measures: definition, computation and applications, Journal of Process Control 10 (2000) 113-123.

[5] T. Schweickhardt, F. Allgower, On system gains, nonlinearity measures, and linear models for nonlinear systems, IEEE Transactions on Automatic Control 54(1) (2009) 62-78.

[6] K.R. Harris, M.C. Colantonio, A. Palazoglu, On the computation of a nonlinearity measure using functional expansions, Chemical Engineering Science 55 (2005) 2393-2400.

[7] D. Sun, K. A. Hoo, Nonlinearity measure for a class of SISO nonlinear systems, International of Journal Control 73 (2000) 29-37.

[8] C.A. Desoer, Y.T. Wang, Foundations of feedback theory for nonlinear dynamical systems, IEEE Trans. Cir. Syst. 27 (1980) 104-123.

[9] Y. Liu, X.R. Li, Measure of nonlinearity for estimation, IEEE Transactions on Signal Processing, 63(9) (2015) 2377-2388.

[10] M. Guay, The effect of process nonlinearity on linear controller performance in discrete-time systems, Computers and Chemical Engineering 30 (2006) 381-391.

[11] S.M. Hosseini, T.A. Johansen, A. Fatehi, Comparison of Nonlinearity Measures based on Time Series Analysis for Nonlinearity Detection, Modeling, Identification and control 32(4) (2011)123-140.

[12] J. Liu, Q. Meng, F. Fang, Minimum variance lower bound ration based nonlinearity measure for closed loop systems, Journal of Process Control 23 (2013) 1097-1107.

[13] G.T. Tan, M. Huzmezan, K.E. Kwok, Vinicombe metric as a closed-loop nonlinearity

measure, European Control Conference, Cambridge, UK, 2003, 751-756.

[14] W. Tan, H.J. Marquez, T. Chen, J. Liu, Analysis and control of a nonlinear boiler-turbine unit, Journal of process control 15 (2005) 883-891.

[15] J. Du, C. Song, P. Li, A Gap metric based nonlinearity measure for chemical processes, Proceedings of the 2009 American Control Conference, St. Louis, MO, US, 2009**,** 4440-4445.

[16] J. Du, Z. Tong, An improved nonlinearity measure based on gap metric, Proceedings of the 33rd Chinese Control Conference, Nanjing, China, 2014, 1920-1923.

[17] T.T. Georgiou, M.C. Smith, Optimal robustness in the gap metric, IEEE Transactions on Automatic Control 35 (6) (1990**)** 673-686.

[18] A.K. El-Sakkary, The gap metric: Robustness of stabilization of feedback systems, IEEE Transaction on Automatic Control 30 (3) (1985) 240-247.

[19] J. Du, T.A. Johansen, Integrated Multimodel Control of Nonlinear Systems Based on Gap Metric and Stability Margin, Industrial and Engineering Chemical Research 53(24) (2014**)** 10206–10215.

[20] J. Du, T.A. Johansen, A gap metric based weighting method for multimodel predictive control of MIMO nonlinear systems, Journal of Process Control 24 (2014) 1346-1357.

[21] E. Arslan, M.C. Camurdan, A. Palazoglu, Y. Arkun, Multimodel Scheduling Control of Nonlinear Systems using Gap Metric, Industrial and Engineering Chemical Research 43(2004) 8274-8283.

[22] R. Jeyasenthil, P.S.V. Nataraj, A multiple model gap-metric based approach to nonlinear quantitative feedback theory, IFAC-PapersOnLine 49-1 (2016) 160-165.

[23] Q. Chi, J. Liang, A multiple model predictive control strategy in the PLS framework, Journal of Process Control 25 (2015**)** 129-141.

[24] J. Du, C. Song, Y. Yao, P. Li, Multilinear model decomposition of MIMO nonlinear systems and its implication for multilinear model-based control, Journal of Process Control 23 (2013) 271-281.

[25] J. Du, C. Song, P. Li, Application of gap metric to model bank determination in multilinear model approach, Journal of Process Control 19 (2009) 231-240.

[26] W. Tan, H.J. Marquez, T. Chen, J. Liu, Multimodel analysis and controller design for nonlinear processes, Comput. Chem. Eng. 28 (2004) 2667-2675.

[27] O. Galán, J.A. Romagnoli, A. Palazoglu, Y. Arkun, Gap metric concept and implication for multilinear model-based controller design, Industrial and Engineering Chemical Research 42 (2003) 2189-2197.

[28] J. Du, C. Song, P. Li, Multimodel control of nonlinear systems: An integrated design procedure based on gap metric and H∞ loop-shaping, Industrial and Engineering Chemical Research 51(2012) 3722-3731.

[29] J. Du, T.A. Johansen, Integrated Multilinear Model Predictive Control of Nonlinear Systems Based on Gap Metric, Industrial and Engineering Chemical Research 54 (22) (2015) 6002–6011.

[30] C. Song, B. Wu, J. Zhao, P. Li, An integrated state space partition and optimal control method of multi-model for nonlinear systems based on hybrid systems, Journal of Process Control 25 (2015) 59-69.

[31] C.R. Porfirio, E.A. Neto, D. Odloak, Multi-model predictive control of an industrial C3/C4 splitter. *Contr. Eng. Pract.* 11 (2003) 764-779.

[32] N.N. Nandola, S. Bhartiya, A multiple model approach for predictive control of nonlinear hybrid systems, Journal of Process Control 18(2008**)** 131-148.

[33] M. Kuure-Kinsey, B.Bequette, Multiple Model Predictive Control Strategy for Disturbance Rejection, Ind. Eng. Chem. Res. 49 (2010) 7983-7989.

[34] M. Garcia, C. Vilas, L. Santos, A. Alonso, A robust multi-model predictive controller for distributed parameter systems, Journal of Process Control 22 (2012) 60-71.

[35] G. Stojanovski, M. Stankovski, G. Dimirovski, Multiple-model model predictive control for high consumption industrial furnaces, FACTA UNIVERSITATIS, Series: Automatic Control and Robotics 9(1) (2010) 131-139.

[36] X. Du, P. Yu, C. Ren, Clustering Multi-model generalized predictive control and its application in wastewater biological treatment Plant, Journal of Applied Sciences 13 (21) (2013) 4869-4874.

[37] X. Tao, D. Li, Y. Wang, N. Li, S. Li, Gap-metric-based multiple-model Predictive control with a polyhedral stability region, Ind. Eng. Chem. Res. 54 (2015) 11319-11329.

[38] K. Zhou, J. Doyle, Essentials of Robust Control, Prentice Hall, Upper Saddle River, New Jersey, 1999.

[39] W.J. Rugh, J.S. Shamma, Research on gain scheduling, Automatica 36 (2000) 1401-1425.

[40] G.L. Plett, Adaptive inverse control of linear and nonlinear systems using dynamic neural networks, IEEE Transactions on Neural Networks 14(2) (2003) 360 - 376.